

MICRO FLOW STANDARD FOR STEADY AND PULSATING FLOW

H. Bissig, M. Tschannen and M. de Huu

Federal Institute of Metrology METAS, Bern-Wabern, Switzerland

ABSTRACT

Micro and nano flow calibrations are important in several applications such as volumetric dosage or drug delivery where the exact amount of the delivered volume or a stable flow rate is crucial for the efficient operation. However, international traceability in the micro and nano flow is not validated up to date in Europe for flow rate ranges below 33 $\mu\text{l}/\text{min}$. METAS develops in the framework of the EMRP project “HLT07 Metrology for Drug Delivery” [1, 2] a primary standard to cover the flow rate range from 1 ml/min down to 100 nl/min with uncertainties in the range from 0.1 % to 0.6 % and calibration of pulsating flow rates from 1 ml/min down to 1 $\mu\text{l}/\text{min}$ with measurement uncertainties from 0.2 % to 2.7 % (coverage factor 95 %).

KEYWORDS

Micro flow, liquid, dynamic gravimetric calibration, pulsating flow

DESIGN OF THE FACILITY

To realize such small flow rates with the appropriate flow rate stability METAS applies the principle of generating the flow by means of a constant pressure drop over a capillary tube according to the law of Hagen-Poiseuille. As shown in Fig. 1 and Fig. 2, a metallic bellow is immersed into a water tank where the water pressure is controlled by expanding or compressing the metallic bellow by means of adjusting the air pressure inside the bellow with a pressure controller. For this part, the air pressure inside the bellow is adjusted according to the signal of a pressure sensor inside the water tank in order to reach the desired water pressure in the tank. The stability of the water pressure is guaranteed by means of a regulation loop controlled by software. The pressure drop from the water tank to the atmospheric pressure at the outlet needle and the size of the capillary tube determine the flow rate.

The facility is designed in such a way that the water pressure upstream the DUT (Device Under Test) can be varied to some extent. In one mode, the water flows from the capillary tube through the DUT and finally in the measurement beaker on the balance. The main pressure drop occurs over the capillary tube and this means that the pressure difference with respect to the ambient pressure upstream the DUT is very small. In a second mode, the water is first guided

through the DUT and then through the capillary tube and in the measurement beaker on the balance. In this case the water pressure upstream the DUT is similar to the water pressure in the water tank.

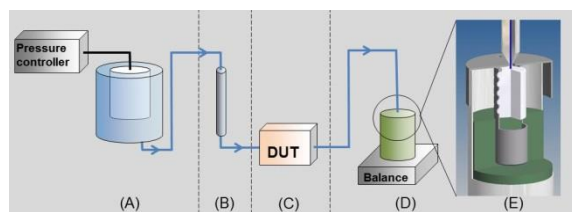


Figure 1: Simplified drawing of the working principle of the facility. (A) water tank with immersed metallic bellow and pressure controller, (B) capillary tube, (C) device under test (DUT), (D) measurement beaker on the balance, (E) detailed cross-section of the top part of the measurement beaker.

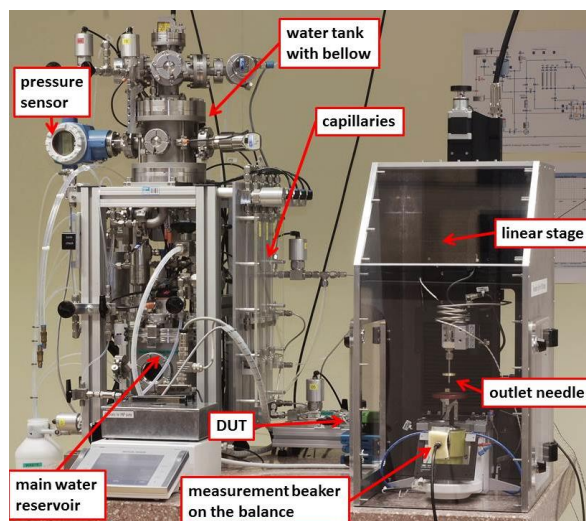


Figure 2: Photograph of the facility with the main components: water tank with metallic bellow, capillary tubes, device under test (DUT), measurement beaker on the balance, main water reservoir.

Evaporation rate

An important issue is the evaporation rate of the water in the beaker during the measurement. To control this process we apply the conventional method of adding water in an evaporation trap in the weighing zone where the air is then saturated with humidity. Additionally, we have built a special measurement beaker as drawn in the detailed cross-section in Fig. 1 (E). The outlet needle is positioned above the glass filter (white disc) where the water enters the measurement beaker. The capillary force in the glass filter sucks the water in before any droplet can be

formed at the surface. The water cleaves its way through the glass filter and continues in the water-absorbing foam into the bulk. This prevents the water to be at the surface. With this setup we get stable evaporation rates of $(3.15 \pm 0.50) \mu\text{g}/\text{min}$ or $(3.16 \pm 0.50) \text{nl}/\text{min}$ respectively and $(3.42 \pm 1.00) \mu\text{g}/\text{min}$ or $(3.43 \pm 1.00) \text{nl}/\text{min}$ respectively depending on the porosity of the glass filters used.

Gravimetric flying start-stop method

The measurements are performed by means of the dynamic gravimetric flying start-stop method. This means that the desired flow rate is set and the data acquisition is only started once the flow rate has reached a steady state. Therefore, the measurement beaker is continuously filled with water and the weighing data are continuously collected with the time stamp of the balance at an acquisition rate of 10 Hz.

Determination of flow rate

The collected weighing data are then fitted by means of the ‘‘Trust-region Levenberg-Marquardt algorithm’’ [3] where the uncertainties in the dependent as well as the independent variable are taken into account. To perform the fit, we use the Software IGOR Pro and the fitting function ‘‘Orthogonal Distance Regression (ODR)’’ [3, 4].

Flow rate determination is best explained using an example. We choose a fixed time window of 23 minutes for the flow rate shown in Fig. 3 as white and light gray portion and perform an ODR linear fit on the collected data. The resulting mass flow rates are then converted to volume flow rates and are shown in Fig. 4 as black empty circle and light gray full triangle with their uncertainties. The time stamp of the determined volume flow rate of each fixed time window is the center time of these data. This guarantees that any strong change in the flow rate is detected at the occurring time independently on the chosen fixed time window. By increasing the starting time of this fixed time window by time steps corresponding to the acquisition rate of 10 Hz we can follow the evolution of the flow rate in time. Applying this to the collected weighing data shown in Fig. 3 we get the evolution in time of the volume flow rate as shown in Fig. 4.

Presentation

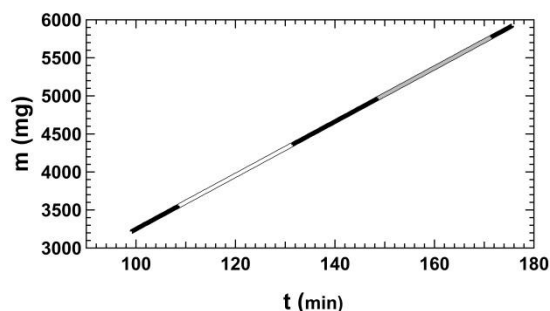


Figure 3: Increase of mass as a function of time. Two time window of 23 minutes are shown in white and light gray.

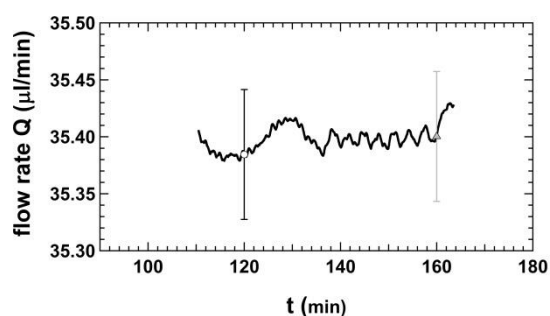


Figure 4: The determined volume flow rate as a function of time. The black empty circle and light gray full triangle are the determined volume flow rates corresponding to the data in the time windows (white and light gray) in Fig. 3.

Flow rate stability

As mentioned in the beginning, the flow rate stability is very important. In Fig. 5, we show the evolution in time of the reference volume flow rate already shown in Fig. 4 and the corresponding data of the DUT (mini Cori-Flow M12P from Bronkhorst, flow rate at 1 % of full scale [5]) where the deviations to the mean reference volume flow rate of $35.42 \mu\text{l}/\text{min}$ are plotted as a function of time. To illustrate the flow rate stability, the uncertainty ($k=2$) of the reference volume flow rate of 0.16 % is added on the Fig. 5 as black dashed lines and we observe the fluctuations being clearly within the uncertainties.

The histograms of the data shown in Fig. 5 are plotted in Fig. 6 in order to better visualize the flow rate stability of the reference volume flow rate as well as the volume flow rate of the DUT. We can clearly observe that the stability is very good and we obtain a distribution with $\sigma = 0.032 \%$ for the reference volume flow rate, as seen in Fig. 6.

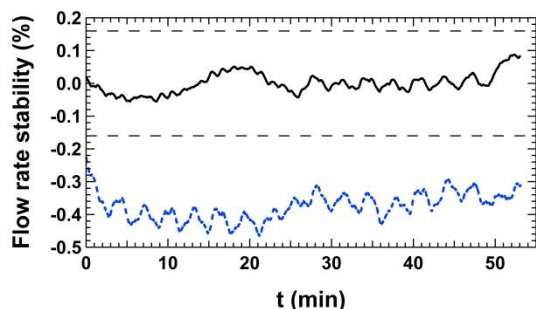


Figure 5: Evolution in time of the relative deviation of the reference volume flow rate (solid black line) from the mean value of $35.42 \mu\text{l}/\text{min}$ and the corresponding relative deviation of the DUT (dotted blue line). To illustrate the flow rate stability, the uncertainty ($k=2$) of the reference volume flow rate of 0.16% (dashed black line) is added where the fluctuations are clearly within the uncertainties.

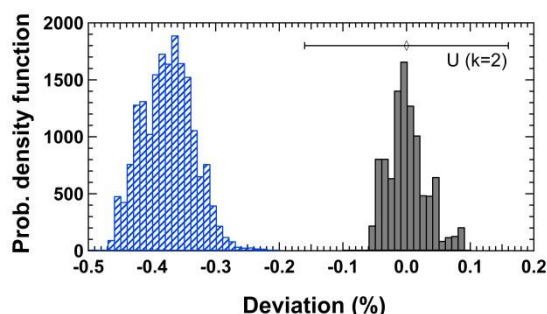


Figure 6: Histogram of the data shown in Fig. 5. (Full dark gray bars) Distribution of the reference volume flow rate with $\sigma = 0.032 \%$ and the corresponding uncertainty ($k=2$) of the reference volume flow rate. (Dashed blue bars) Distribution of the volume flow rate of the DUT.

CALIBRATION OF FLOW METER IN STEADY FLOW

In Fig. 7 and 8, calibration results for steady flow of commercially available Coriolis flow meters and thermal flow meters are shown, which highlight the repeatability and the reproducibility of the facility.

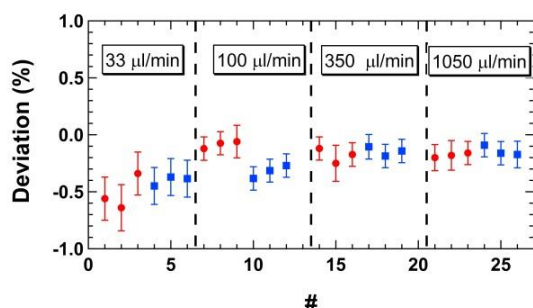


Figure 7: Calibration of a commercially available Coriolis flow meter “mini Cori-Flow M12P” from Bronkhorst High-Tech B.V. [5]. The red circles and the blue squares represent repeatability measurements whereas the different color codes represent the reproducibility measurements in the flow rate range from $1 \text{ ml}/\text{min}$ to $33 \mu\text{l}/\text{min}$.

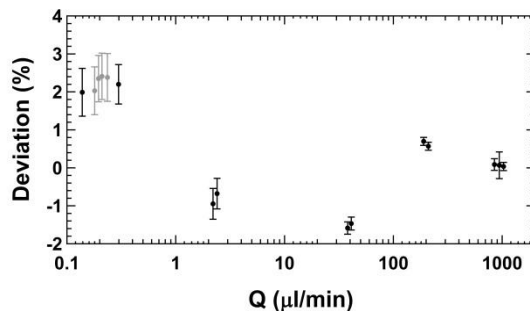


Figure 8: Calibration of commercially available thermal flow meters “SLG1430-025”, “SLI-0430” and “SLI-1000” from Sensirion AG [6]. The black and gray full circles represent repeatability measurements whereas the different color codes in the range of $0.1 \mu\text{l}/\text{min}$ to $0.3 \mu\text{l}/\text{min}$ represent the reproducibility measurements in this flow rate range.

CALIBRATION AT PULSATING FLOW

Furthermore, the facility can generate unsteady flow by means of varying the water pressure in the water tank according to a desired pattern. This enables us to calibrate flow sensors under unsteady flow conditions in the flow rate range of $1 \text{ ml}/\text{min}$ down to $1 \mu\text{l}/\text{min}$.

Moreover, flow generators can be connected to the facility and calibrated in the same way. In Fig. 9, three calibration curves of a commercially available syringe pump are shown. The selected flow rate at the syringe pump is $100 \mu\text{l}/\text{min}$ and the instantaneous deviations to the reference flow rates are reported as a function of the syringe plunger position.

A reoccurring pattern of pulsating flow can be observed (highlighted in gray) where the cycles correspond to full rotations of the spindle of the syringe pump.

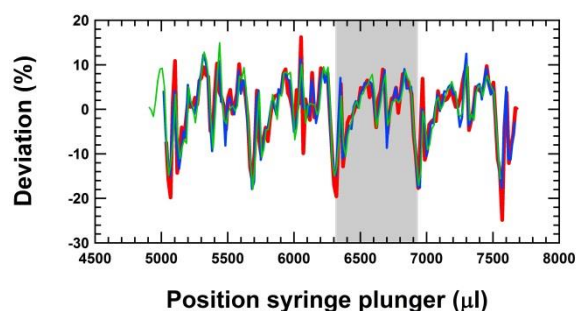


Figure 9: Three calibration curves of a commercially available syringe pump (NEXUS 3000 [7]) at the selected flow rate of $100 \mu\text{l}/\text{min}$. The instantaneous deviations to the reference flow rates are reported as a function of the syringe plunger position. The reoccurring pattern of pulsating flow due to the full rotation of the spindle is highlighted in gray.

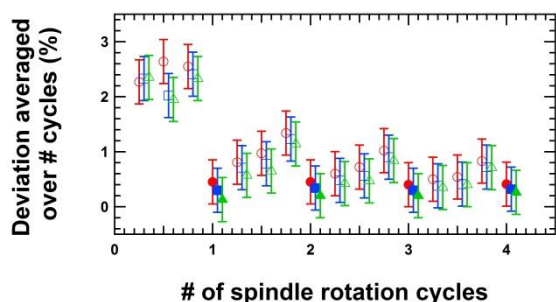


Figure 10: Mean deviation averaged over fractional value of spindle rotation cycles starting from the syringe plunger position of 7550 μl . The red circles, the blue squares and the green triangles are the mean deviations from the corresponding data shown in Fig. 9. Full symbols correspond to integer numbers of the spindle rotation cycles, whereas the empty symbols represent fractional values of spindle rotation cycles. The blue squares are shifted by 0.05 and the green triangles are shifted by 0.10 in the x-axis for clarity.

The average flow rate or the average deviation is then determined over an integer number of these cycles. To illustrate the significance of the average over an integer number of spindle rotation cycles, we show in Fig. 10 the averaged deviation as a function of the fractional value of the spindle rotation cycles starting from the syringe plunger position of 7550 μl . The red circles, the blue squares and the green triangles are the mean deviations from the corresponding data shown in Fig. 9. Full symbols correspond to integer numbers of the spindle rotation cycles, whereas the empty symbols represent fractional values of spindle rotation cycles. The blue squares are shifted by 0.05 and the green triangles are shifted by 0.10 in the x-axis for clarity. We can observe that the average over an integer value of the spindle rotation time leads to reproducible deviations, whereas fractional values of spindle rotation cycles can lead to erroneous deviations. Obviously, if the fractional value of spindle rotation cycles becomes larger, the erroneous discrepancy becomes smaller, even within the stated uncertainty of 0.4 % for this case.

CONCLUSIONS

The micro flow facility at METAS is developed to perform calibrations of steady flow rates from 1 ml/min down to 100 nl/min with measurement uncertainties from 0.1 % to 0.6 % and calibration of pulsating flow rates from 1 ml/min down to 1 $\mu\text{l}/\text{min}$ with measurement uncertainties from 0.2 % to 2.7 %.

The flow rate range from 1 ml/min down to 10 $\mu\text{l}/\text{min}$ has already been validated by means of an inter-comparison within the EMRP project [2, 8]. The lower flow rate range from 10 $\mu\text{l}/\text{min}$ down to 100

nl/min is currently in the validation process where a research inter-comparison takes place within Euramet [9].

So far promising results of repeatability and reproducibility measurements of Coriolis and thermal flow meters as well as flow generators have been reported.

ACKNOWLEDGEMENT

The EMRP project “HLT07 Metrology for Drug Delivery” is carried out with funding by the European Union under the EMRP. The EMRP is jointly funded by the EMRP participating countries within EURAMET and the European Union.

REFERENCES

- [1] EMRP Call 2011 - Health, SI Broader Scope & New Technologies, HLT07 Metrology for drug delivery, www.euramet.org
- [2] Website of the EMRP Project HLT07 MeDD, <http://www.drugmetrology.com/>
- [3] IGOR Pro, WaveMetrics Inc., Version 6.21, ODRPACK95, Manual Version 6.21, Volume III, p. 229 Curve Fitting References
- [4] W. Press, S. Teukolsky, W. Vetterling, B. Flannery, Numerical Recipes in C, New York: Cambridge University Press, 1992, ch. 15.3 Straight-Line Data with Errors in Both Coordinates, pp. 666 – 670, ch. 15.5 Nonlinear Models – Levenberg-Marquardt Method, pp. 681 – 688.
- [5] Bronkhorst High-Tech B.V., www.bronkhorst.com
- [6] Sensirion AG, www.sensirion.com
- [7] Chemyx Datasheet NEXUS 3000 syringe pump, Chemyx Inc. www.chemyx.com
- [8] Christopher David, Claus Melvad, Hugo Bissig and Elsa Batista. Research inter-comparison for small liquid flow rates (2 g/h to 600 g/h). Proceedings of Flomeko 2013, A10.4 – 314.
- [9] Euramet, TC-F Projects, research inter-comparison E-1291. Comparison between recently developed primary standards. www.euramet.org

CONTACT

* H. Bissig, Hugo.Bissig@metas.ch